

Investigating the Effects of Strain on Silicon MOSFETs

Final Project, EE 531

Bart Trzynadlowski

March 17, 2007

Objective

Strain engineering has been used in recent years to improve the performance of nanoscale devices. It is a technique which I feel is not immediately obvious to people (such as myself) who have not studied solid state physics in sufficient detail to appreciate the effect of mechanical strain on electrical conductivity. Therefore, I have decided to investigate strained silicon so that I can understand its impact on MOSFET characteristics studied in this course, namely the drain current.

1. Effects of Strain on Mobility

The expressions for MOSFET drain current, as functions of terminal voltages, take the form:

$$I_D = \mu_{eff} \cdot F(V_{GS}, V_{DS}, V_{SB})$$

F varies for different regions of device operation and approximations made to calculate the current. It is also dependent on device and environmental parameters including doping, temperature, and material constants. The μ_{eff} term is the effective mobility of carriers in the MOSFET channel: electrons for NMOS devices and holes for PMOS. It is influenced by scattering processes and conduction effective mass.

The direction relationship between mobility and current is obvious. A higher mobility is desirable.

Conduction Band Minima

Applying strain to a material will change the spacing of the atoms and thus the characteristics of the energy bands because they are dependent on the periodicity and spacing of the lattice structure.

In k-space, the Si conduction band has six elliptical minima as shown in Fig. 1.1.

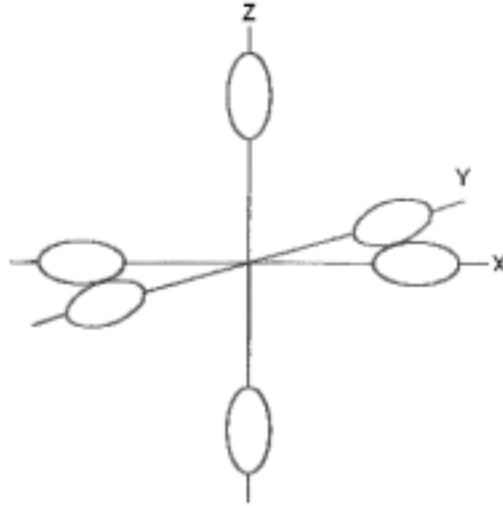


Fig. 1.1: Visualization of energy band minima in Si k-space.^[1]

Under relaxed conditions, the minima are symmetric – their energies are equal and so are their electron populations. The effective mass of the electrons is different depending on whether they are in a minimum aligned with (longitudinal) or perpendicular (transverse) to the applied electric field. Effective mass in general is defined in terms of a tensor:

$$m_{ij}^* = \hbar^2 \left(\frac{\partial E}{\partial k_i \partial k_j} \right)^{-1}$$

The i and j subscripts correspond to each of the X, Y, Z axes. The effective mass is dependent on the curvature of the bands at the point in k-space where the electron is located. The conduction effective mass (the scalar effective mass in the direction of conduction used in mobility and transport-related equations), when unstrained, is:

$$m_{cond}^* = \frac{3}{(m_l^{-1} + 2m_t^{-1})}$$

Altering the populations in the minima will increase or decrease this effective mass. It is favorable to increase the population in the four transverse valleys because m_t is the lower effective mass. Changing the minimum energy levels will change the population at those levels by a factor of $\exp\left(\frac{\Delta E}{kT}\right)$.

It so happens that tensile strain along one axis will break the degeneracy of the minima by lowering the energy of the four transverse minima (with lower effective mass) and raising the energy of the two longitudinal minima as shown in Fig. 1.2.

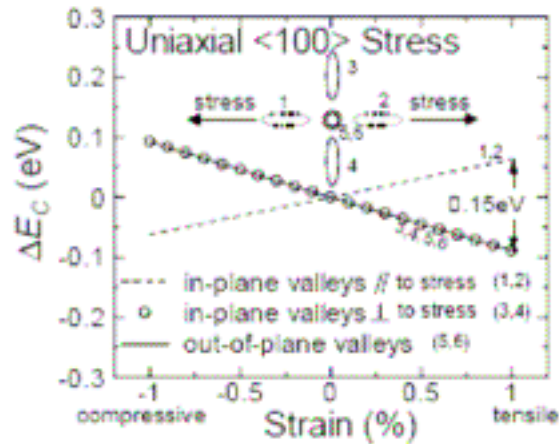


Fig. 1.2: Breaking of the degeneracy due to strain.^[2]

Compressive strain has the opposite effect. Tensile strain is generally favorable when the majority carriers are electrons, such as in n-channel MOSFETs. The effect of strain in the linear elastic regime on energy band curvature is assumed to be negligible.

Valence Bands

A similar process occurs in the valence bands. A key difference is that shape of the bands is deformed under stress. Fig. 1.3 shows the heavy hole band under a variety of conditions.

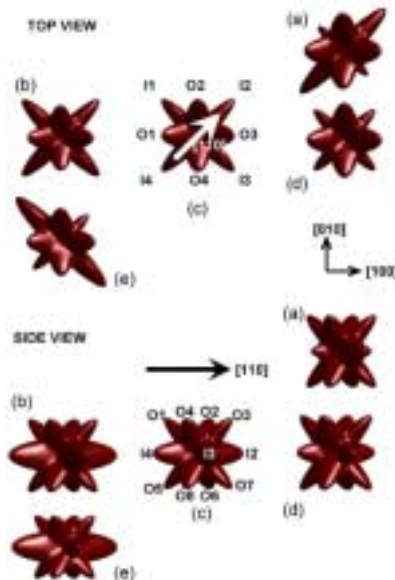


Fig. 1.3: Top and side views of the heavy hole band surface at 100 meV. (a) Tensile stress along [110], 1 GPa. (b) Biaxial compressive stress, 1 GPa. (c) No stress. (d) Biaxial tensile stress, 1 GPa. (e) Compressive stress along [110], 1 GPa.^[3]

The analysis for holes is therefore more complex and for the purposes of simulation, simplified models are used. In general, appropriately directed compressive strain is

favorable for hole transport. Due to time constraints, this report focuses on the effects of strain in n-channel devices.

2. Implementation of Strained Silicon Devices

Several different techniques for inducing strain in MOSFET channels have been developed. A few specific cases are examined here. In each case, the strains considered are relatively small and safely within the linear elastic region.

Biaxial Stress on a Thin Film

Growing a thin film epitaxially upon a much thicker substrate will tend to force the film to line up with the underlying lattice. If a mismatch in the lattice constants exists, either compressive or tensile strain will be induced depending on whether the thin film lattice constant is larger or smaller, respectively. Fig. 2.1 illustrates Si conforming to an SiGe alloy with a wider-spaced lattice.

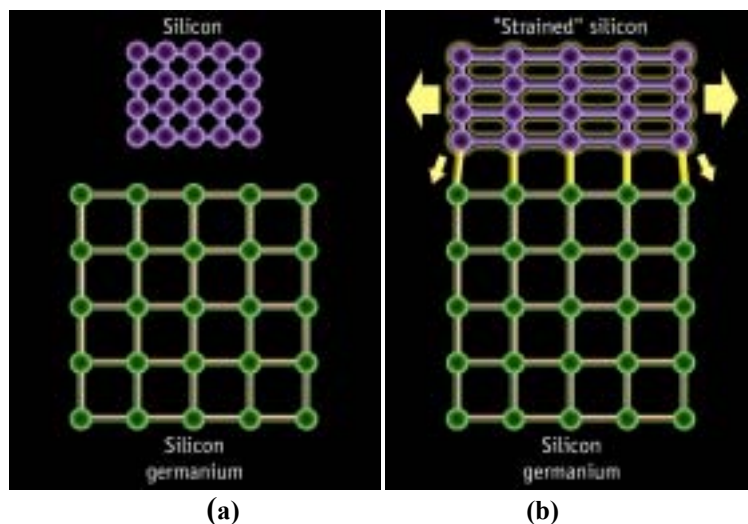


Fig. 2.1: (a) Si lattice constant is smaller than SiGe. (b) Depositing Si causes it to “stretch” in order to align with underlying material.^[4]

For NMOS transistors, tensile stress in the channel is desirable. Fig. 2.2 is an image of an IBM device with a thin-film Si layer which forms the channel region grown on top of a thicker SiGe region with 15% Ge concentration.

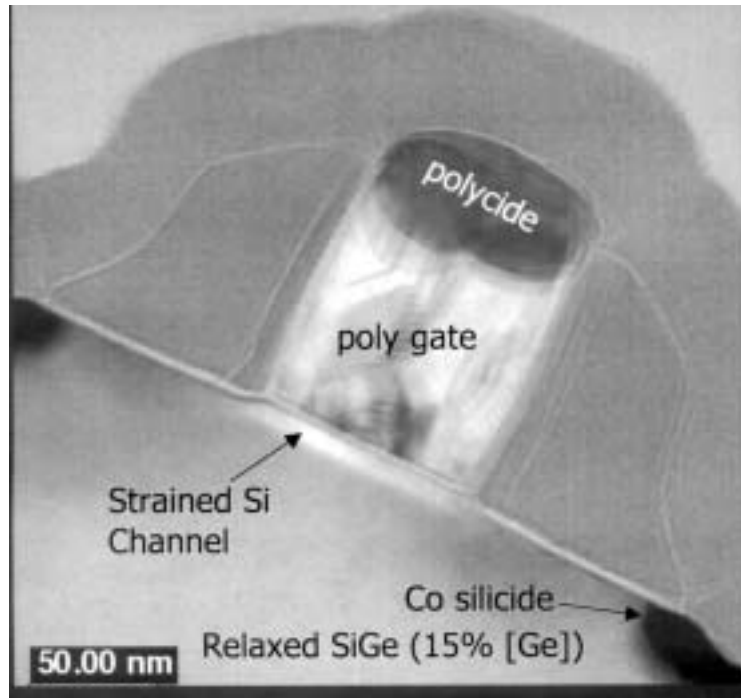


Fig. 2.2: Cross-section of an NMOS FET with tensile strain in the channel. ^[4]

In order to investigate biaxial stress with simulation, a simplified model was developed to compute the stresses in such a system. A schematic representation of the system is shown in Fig. 2.3. The constraints are as follows:

- The Si lattice must match the spacing of the SiGe lattice in the X and Z directions. This gives us ϵ_{xx} and ϵ_{zz} .
- Stress in the Y direction, σ_{yy} , is 0 since there is nothing to apply it although there will be an unknown strain.

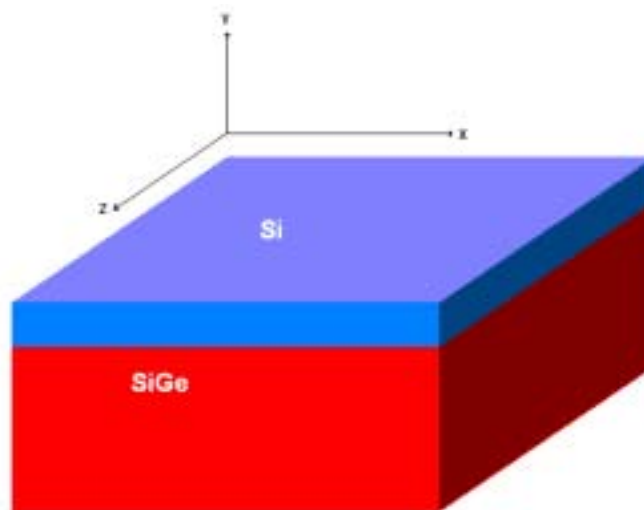


Fig. 2.3: Si thin film conforms to underlying SiGe thereby creating tension.

This results in three known quantities (ϵ_{xx} , ϵ_{zz} , σ_{yy}) and three unknowns (ϵ_{yy} , σ_{xx} , σ_{zz}). Shear stresses are assumed to be negligible and set to 0. The stresses and strains are related with a matrix equation:

$$\begin{bmatrix} \epsilon_{xx} \\ \epsilon_{yy} \\ \epsilon_{zz} \end{bmatrix} = \begin{bmatrix} s_{11} & s_{12} & s_{12} \\ s_{12} & s_{11} & s_{12} \\ s_{12} & s_{12} & s_{11} \end{bmatrix} \begin{bmatrix} \sigma_{xx} \\ \sigma_{yy} \\ \sigma_{zz} \end{bmatrix}$$

The stiffness coefficients for Si are shown in Table 2.1. The same matrix is also used for SiGe for convenience although in reality, it will be slightly different depending on the Ge concentration.

Table 2.1: Coefficients of the stiffness matrix of Si.^[4]

| S₁₁ | S₁₂ |
|---|--|
| $0.768 \times 10^{-12} \text{ cm}^2/\text{dyn}$ | $-0.214 \times 10^{-12} \text{ cm}^2/\text{dyn}$ |

A thin film grown on top of a substrate with a different lattice constant will attempt to line up with the lattice sites below, inducing strain:

$$\epsilon = \frac{a_{\text{film}} - a_{\text{substrate}}}{a_{\text{substrate}}}$$

Here, a_{film} and $a_{\text{substrate}}$ are the lattice constants of the film and substrate material, respectively^[5].

Example: Si on Si_{0.85}Ge_{0.15}

The stresses and strains on the Si channel in the NMOS device pictured in Fig. 2.2 can be calculated with the prescription given above.

Known:

$$\begin{aligned} a_{\text{Si}} &= 5.431 \text{ \AA} \\ a_{\text{SiGe}}(x) &= 5.431 + 0.20x + 0.027x^2 \text{ \AA for Si}_{1-x}\text{Ge}_x. \\ \epsilon_{xx} = \epsilon_{zz} &= \frac{a_{\text{SiGe}}(0.15) - a_{\text{Si}}}{a_{\text{SiGe}}(0.15)} = 5.676 \times 10^{-3} \\ \sigma_{yy} &= 0 \end{aligned}$$

Unknown:

$$\sigma_{xx}, \sigma_{zz}, \epsilon_{yy}$$

Solve:

$$\begin{bmatrix} 5.676 \times 10^{-3} \\ \epsilon_{yy} \\ 5.676 \times 10^{-3} \end{bmatrix} = \begin{bmatrix} s_{11} & s_{12} & s_{12} \\ s_{12} & s_{11} & s_{12} \\ s_{12} & s_{12} & s_{11} \end{bmatrix} \begin{bmatrix} \sigma_{xx} \\ 0 \\ \sigma_{zz} \end{bmatrix}$$

$$\sigma_{xx} = 1.025 \times 10^{10} \text{ cm}^2/\text{dyn} = 1.025 \text{ GPa}$$

$$\sigma_{zz} = 1.025 \text{ GPa}$$

$$\epsilon_{yy} = -4.385 \times 10^{-3}$$

The effect on mobility will be computed using Sentaurus with this data further below.

Uniaxial Stress

Uniaxial stress techniques attempt to control the stress in a single primary direction with negligible stress and strain in the perpendicular directions. There are several ways of implementing this. One common technique for generating uniaxial compression in the channel (which is helpful for PMOS devices) is to use SiGe in the source and drain regions which will attempt to expand thereby exerting compression on the Si channel in between them, as shown in Fig. 2.4.

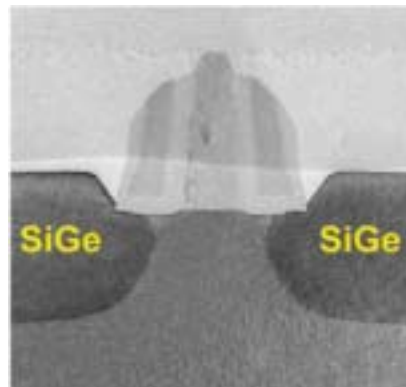


Fig. 2.4: SiGe in source and drain regions induces compressive strain in the channel.

Four-point bending, as shown in Fig. 2.5, physically deforms the wafer (or a thin strip thereof) inducing compressive and tensile strains at different depths. Other mechanisms exist for straining wafers and integrated circuit dies after they have already been processed.



Fig. 2.5: Four-point bending of a wafer in between two plates and four contact points.^[2]

Layers of nitride material grown over the top of devices can be used to create either tensile or compressive strain. This process is especially well suited for CMOS devices and has been employed by IBM, as illustrated in Fig. 2.6. Intel has introduced a similar technique in its 90 nm process node which uses a tensile nitride for NMOS devices but uses SiGe in the source and drain to create compression in the PMOS channels.^[6]

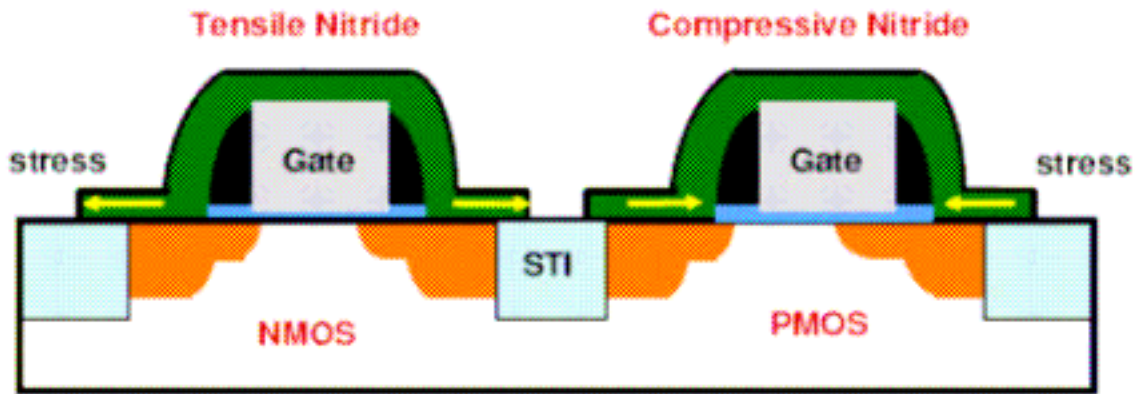


Fig. 2.6: Nitride caps in an IBM CMOS process.^[6]

Example: Compression Due to SiGe Source and Drain Regions

In order to investigate the effects of SiGe source and drain regions, the simple model of Fig. 2.7 was analyzed.

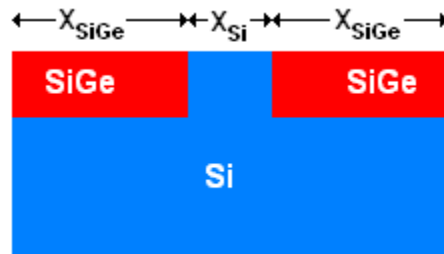


Fig. 2.7: Simplified model of SiGe in source and drain regions.

The source and drain regions are created using long strips of SiGe which are several times the length of the Si channel region in between. The constraints on such a system are:

- Averaged over one period (one SiGe strip and one Si strip), the strained regions must conform to the Si substrate underneath.
- The SiGe strips must conform to the underlying Si lattice in the Z direction thereby creating a known strain. The Z strain component for the Si region will be 0 because there is no lattice mismatch.
- No stress is exerted on either region in the Y direction – there is nothing with which to exert a force.
- The stress exerted in the X direction on the SiGe region is equal to that exerted on the Si region (Newton’s Third Law.)

This initially results in four known quantities (Z strain and Y stress in both regions) and eight unknowns (the X and Y strains and stresses in each region.) This can be reduced to seven unknowns given that the X stresses must be equal. Besides the two stress-strain matrix relations (one for each region), the conformance of each region to the Si substrate underneath allows a seventh equation to be formulated:

$$\left(1 + \epsilon_{xx}^{SiGe}\right) \left(x_{SiGe} \frac{a_{SiGe}}{a_{Si}}\right) + \left(1 + \epsilon_{xx}^{Si}\right) x_{Si} = x_{SiGe} + x_{Si}$$

The width of each SiGe region, were it totally relaxed, would be

$$W = x_{SiGe} \frac{a_{SiGe}}{a_{Si}}$$

This is because that when grown on top of the Si substrate, it will attempt to align itself with the smaller lattice underneath. Without this constraint, the same strip of SiGe would naturally want to expand by a factor of a_{SiGe}/a_{Si} . The $(1+\epsilon_{xx})$ terms serve to add the strain distance to each region, thereby creating an equation where the strains are balanced such that the total width is unchanged.

Given a hypothetical situation where the source and drain regions are composed of 25% Ge and are four times as wide as the Si channel,

$$\begin{aligned} x_{SiGe} &= 4 \text{ units} \\ x_{Si} &= 1 \text{ unit} \\ \frac{a_{SiGe}(0.25)}{a_{Si}} &= 1.00957 \\ \frac{a_{Si} - a_{SiGe}(0.25)}{a_{Si}} &= -9.484 \times 10^{-3} \end{aligned}$$

The following are known:

$$\begin{aligned} \epsilon_{zz}^{SiGe} &= -9.484 \times 10^{-3} \\ \epsilon_{zz}^{Si} &= 0 \\ \sigma_{yy}^{SiGe} &= 0 \\ \sigma_{yy}^{Si} &= 0 \end{aligned}$$

The system of equations to solve is:

$$\begin{bmatrix} \epsilon_{xx}^{SiGe} \\ \epsilon_{yy}^{SiGe} \\ -9.484 \times 10^{-3} \end{bmatrix} = \begin{bmatrix} s_{11} & s_{12} & s_{12} \\ s_{12} & s_{11} & s_{12} \\ s_{12} & s_{12} & s_{11} \end{bmatrix} \begin{bmatrix} \sigma_{xx}^{SiGe} \\ 0 \\ \sigma_{zz}^{SiGe} \end{bmatrix}$$

$$\begin{bmatrix} \epsilon_{xx}^{Si} \\ \epsilon_{yy}^{Si} \\ 0 \end{bmatrix} = \begin{bmatrix} s_{11} & s_{12} & s_{12} \\ s_{12} & s_{11} & s_{12} \\ s_{12} & s_{12} & s_{11} \end{bmatrix} \begin{bmatrix} \sigma_{xx}^{Si} \\ 0 \\ \sigma_{zz}^{Si} \end{bmatrix}$$

$$(1 + \epsilon_{xx}^{SiGe})(4 \times 1.00957) + (1 + \epsilon_{xx}^{Si})(1) = 1 + 4$$

$$\sigma_{xx}^{SiGe} = \sigma_{xx}^{Si}$$

And the solution is:

$$\epsilon_{xx}^{SiGe} = -7.07 \times 10^{-3}$$

$$\epsilon_{yy}^{SiGe} = 6.43 \times 10^{-3}$$

$$\sigma_{xx}^{SiGe} = \sigma_{xx}^{Si} = -1.37 \times 10^{10} \text{ dyn/cm}^2 = -1.37 \text{ GPa}$$

$$\sigma_{zz}^{SiGe} = -1.63 \times 10^{10} \text{ dyn/cm}^2 = -1.63 \text{ GPa}$$

$$\sigma_{xx}^{Si} = -3.83 \times 10^9 \text{ dyn/cm}^2 = -0.383 \text{ GPa}$$

This model is overly simplified because it does not take into account the actual irregular geometries of the strips and assumes that the stresses and strains are uniform over each region, which is not the case. However, for the purposes of obtaining “ballpark” estimates, it will have to suffice.

Example: Strain Due to Four-Point Bending

Uniaxial stress due to physical bending of the wafer is investigated because data was found that can be compared against using simulations (which will be performed further on.) It is assumed that there is stress only along one axis with the others being 0. This may not be completely accurate but it does allow for an estimate of primary stress component as well as the two perpendicular strain components given only a single strain value along the primary direction. For the case where the uniaxial stress is applied along the X axis and the value of ϵ_{xx} is known to be ϵ_{xx}' , the following system can be used:

$$\begin{bmatrix} \epsilon_{xx}' \\ \epsilon_{yy} \\ \epsilon_{zz} \end{bmatrix} = \begin{bmatrix} s_{11} & s_{12} & s_{12} \\ s_{12} & s_{11} & s_{12} \\ s_{12} & s_{12} & s_{11} \end{bmatrix} \begin{bmatrix} \sigma_{xx} \\ 0 \\ 0 \end{bmatrix}$$

Table 2.2 tabulates the results. Strains shown in bold are known.

Table 2.2: Strains and associated stresses for four-point bending. Known strains are in bold.

| ϵ_{xx} | ϵ_{yy} | ϵ_{zz} | σ_{xx} (Pa) | σ_{yy} | σ_{zz} (Pa) |
|---|-------------------------|---|--------------------|---------------|--------------------|
| 0.02×10^{-2} | -5.57×10^{-5} | -5.57×10^{-5} | 2.60×10^7 | 0 | 0 |
| 0.04×10^{-2} | -1.115×10^{-4} | -1.115×10^{-4} | 5.21×10^7 | 0 | 0 |
| 0.07×10^{-2} | -1.951×10^{-4} | -1.951×10^{-4} | 9.12×10^7 | 0 | 0 |
| -5.57×10^{-5} | -5.57×10^{-5} | 0.02×10^{-2} | 0 | 0 | 2.60×10^7 |
| -1.115×10^{-4} | -1.115×10^{-4} | 0.04×10^{-2} | 0 | 0 | 5.21×10^7 |
| -1.951×10^{-4} | -1.951×10^{-4} | 0.07×10^{-2} | 0 | 0 | 9.12×10^7 |

3. Modeling the Strain Effect in Sentaurus

Sentaurus provides support for modeling mechanical strain. The models it uses are relatively simple and take applied stress as their input. In reality, stress varies throughout the device and Sentaurus supports this with files which specify stresses throughout the system with whatever level of granularity the user defines.

Deformation of the Band Structure

Deformation potential theory describes how the energy bands change due to deformations of the lattice structure due to small strains. The change of the energy in a carrier subvalley is assumed to be linearly proportional to the strain. Sentaurus combines the expressions for change in the carrier subvalley energy levels for holes and electrons into a single expression:

$$\Delta E_{B,i} = \zeta_{i1}^{B2} \epsilon_{11} + \zeta_{i2}^{B2} \epsilon_{22} + \zeta_{i3}^{B2} \epsilon_{33} + \zeta_{i4}^{B2} \sqrt{\frac{(\zeta_{i1}^{B2})^2}{2} ((\epsilon_{11} - \epsilon_{22})^2 + (\epsilon_{22} - \epsilon_{33})^2 + (\epsilon_{11} - \epsilon_{33})^2) + (\zeta_{i1}^{B2})^2 (\epsilon_{11}^2 + \epsilon_{22}^2 + \epsilon_{33}^2)}$$

Where B is C for the conduction band and V for the valence band (this determines which deformation potential matrix, specified by the user or supplied by Sentaurus, is used for the ζ terms.) The square root term only affects the valence band calculations and will be 0 for conduction terms.

Sentaurus does not modify the effective masses but instead uses the averaged values of conduction and valence band energy shift:

$$\frac{\Delta E_B}{kT} = -\ln \left[\frac{1}{n_B} \sum_{i=1}^{n_B} \exp \left(\frac{-\Delta E_{B,i}}{kT} \right) \right]$$

Where n_B is the number of subvalleys in the valence band (n_V) or conduction band (n_C). For Si, these values are 2 (heavy and light hole bands) and 3 (for the six conduction band minima, which come in three symmetric pairs), respectively.^[7]

Strain-induced Mobility Model

With the deformation potential modeled as described above, Sentaurus uses the results as an input to its strain-induced mobility model which computes mobility using the following expressions, if Boltzmann statistics are enabled:

$$\mu_{ii}^n = \mu_n^0 \left[1 + \frac{1 - m_{nl} / m_{nt}}{1 + 2(m_{nl} / m_{nt})} \left(\exp\left(\frac{\Delta E_C - \Delta E_{C,i}}{kT}\right) - 1 \right) \right]$$

$$\mu^p = \mu_p^0 \left[1 + \left(\frac{\mu_{pl}^0}{\mu_p^0} - 1 \right) \frac{(m_{pl} / m_{ph})^{3/2}}{1 + (m_{pl} / m_{ph})^{3/2}} \left(\exp\left(\frac{\Delta E_{V,l} - \Delta E_{V,h}}{kT}\right) - 1 \right) \right]$$

Where m_{nl}/m_{nt} is the ratio of the longitudinal to transverse effective masses of electrons and m_{pl}/m_{ph} is the ratio of effective masses of holes in the light and heavy holes.^[7]

Hole Mobility Models

The effects of strain on the valence bands are more complex than the linear expressions for the conduction band. Multiple options exist for modeling this effect in Sentaurus, including the method described earlier. Sentaurus includes a mobility model for holes proposed by Intel which can be enabled independent of the conduction band model. This model was originally developed considering a 2D model of the valence bands where the upper and lower valleys were assumed to be elliptical. In the unstrained condition, electrons occupy both the high and the low valley. Under stress, splitting of the energy levels would occur. The model was generalized to three dimensions in Sentaurus by assuming that the valence band is a sum of six ellipsoids.^[7]

Unfortunately, due to time constraints, the treatment of holes and PMOS devices in this project is regrettably limited.

Suggested Improvements

The models in Sentaurus are fairly good but there is always room for improvement. The most obvious candidates are the hole models which may benefit from more sophisticated modeling of the valence band curvature deformation due to strain.

It also appears that strain effects on impurities are not considered and as devices become ever smaller, they might become increasingly important to consider.

4. Simulations

Simulations were conducted with Sentaurus Device. Due to difficulties with the SDE and Mdraw structure editors, the n-channel MOSFET from the “simple_Id-Vg” was used. Although this is not a very short channel device, which means the applied stresses would not in reality penetrate throughout the entire channel, the assumption is that these simulations apply to short channel devices where this is true.

The basic structure of the command file is shown in Appendix A. In all cases, the channel lies along the X axis and the direction corresponding to the width (W) of the transistor is Z.

Cases 1, 2, and 3 correspond to the examples provided earlier in this report.

Case 1: Biaxial Tension, Si on Si_{0.85}Ge_{0.15}

In this case, σ_{xx} and σ_{zz} were 1.025 GPa. A plot of the resulting I_{ds} - V_{ds} curves for the unstrained and strained cases is shown in Fig. 4.1. $\mu_{strained}/\mu_{unstrained}$ is 1.33 in this case. As expected, tensile strain enhanced mobility; in this case, the improvement was 33%.

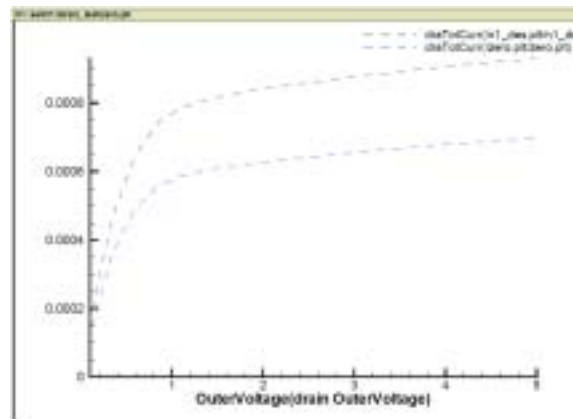


Fig. 4.1: Biaxial tension. The blue curve is for the unstrained case.

Case 2: Uniaxial Compression Due to Si_{0.75}Ge_{0.25} Source and Drain Regions

Here, σ_{xx} and σ_{zz} were -1.37 GPa and -383 MPa, respectively. Fig. 4.2 confirms that the mobility is lowered, as expected. In this case, $\mu_{strained}/\mu_{unstrained}$ is 0.33.

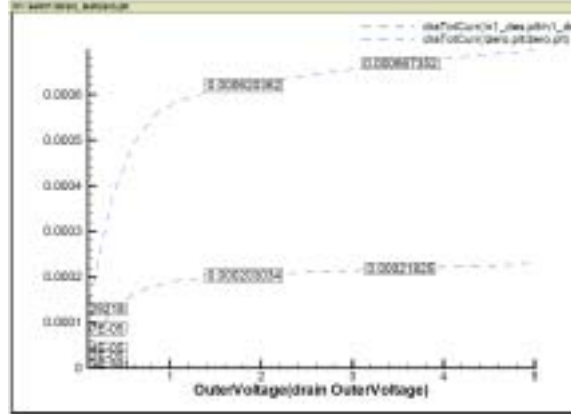


Fig. 4.2: Uniaxial compression. The blue curve is for the unstrained case.

Case 3: Uniaxial Strain Due to Four-Point Bending

This case is particularly interesting because the simulations can be compared with actual data (Uchida, et al.) Table 2.2 lists the stresses and strains for the various conditions tested. Table 4.1 shows the results and compares them with data from Uchida, et al. The experimental data is shown in Fig. 4.3. In the case of the simulations, the parallel axis is X and Z is used as the perpendicular axis.

Table 4.1: Comparison of uniaxial strain simulation with four-point bending data.

| Strain | Simulated $\Delta\mu_{\text{strained}}/\mu_{\text{unstrained}}$ | Experimental Data $\Delta\mu_{\text{strained}}/\mu_{\text{unstrained}}^{[2]}$ |
|--|--|--|
| $\epsilon_{\text{parallel}} = 0.02\%$ | 0.02 | ~ 0.02 |
| $\epsilon_{\text{parallel}} = 0.04\%$ | 0.04 | ~ 0.045 |
| $\epsilon_{\text{parallel}} = 0.07\%$ | 0.07 | ~ 0.075 |
| $\epsilon_{\text{perpendicular}} = 0.02\%$ | -0.011 | ~ 0.01 |
| $\epsilon_{\text{perpendicular}} = 0.04\%$ | -0.0214 | ~ 0.015 |
| $\epsilon_{\text{perpendicular}} = 0.07\%$ | -0.0363 | ~ 0.02 |

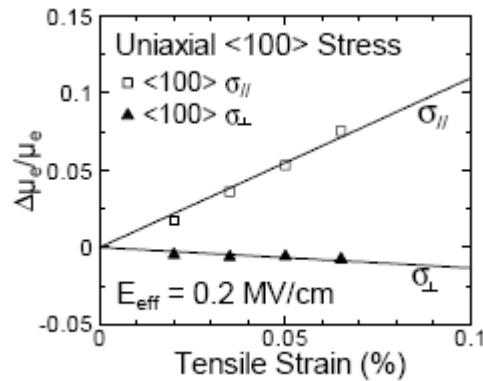


Fig. 4.3: Data from Uchida, et al.^[2]

The data agrees particularly well for tensile strain.

In order to confirm my understanding of the Sentaurus strain model as described earlier, I took the case of 0.02% strain in the X direction and computed what the mobility improvement should have been:

$$\begin{aligned}
\varepsilon_{xx} &= s_{11}\sigma_{xx} = 0.77 \times 10^{-12} (2.6 \times 10^8) = 2.002 \times 10^{-4} \\
\varepsilon_{yy} = \varepsilon_{zz} &= s_{12}\sigma_{xx} = -0.21 \times 10^{-12} (2.6 \times 10^8) = -5.46 \times 10^{-5} \\
\Delta E_{C,1} &= \xi_{11}^{C2} \varepsilon_{11} = 1.8018 \times 10^{-4} \\
\Delta E_{C,2} = \Delta E_{C,3} &= \xi_{21}^{C2} \varepsilon_{11} = -1.72172 \times 10^{-3} \\
\Delta E_C &= -kT \cdot \ln \left[\frac{1}{3} \left[\exp\left(\frac{-1.8018 \times 10^{-4}}{kT}\right) + 2 \exp\left(\frac{-1.72172 \times 10^{-3}}{kT}\right) \right] \right] \\
&= 1.976 \times 10^{-3} \text{ eV} \\
\frac{\mu_{11}^n}{\mu_n^0} &= 1 + \frac{1 - 4.81}{1 + 2(4.81)} \left[\exp\left(\frac{1.1976 \times 10^{-3} - 1.8018 \times 10^{-4}}{kT}\right) - 1 \right] = 1.0144
\end{aligned}$$

Additional Hypothetical Cases

A number of simulations were run with idealized strain cases. The strains were fixed and the required stresses (disregarding physical mechanisms to implement them) were computed. The results are shown in Table 4.2. As is expected, tensile stress along the channel (X) improved mobility whereas compressive strain hindered it. Biaxial strain was also very helpful provided that at least one of the strained directions was along the channel. The results show that biaxial strain in both perpendicular directions reduces mobility. This is because the subvalleys with the longitudinal mass will be decreased the most, and therefore will become the most heavily occupied, and the effective mass in that direction is the highest. Mobility is inversely proportional to conduction effective mass.

Table 4.2: Simulations of various strain conditions.

| ε_{xx} | ε_{yy} | ε_{zz} | σ_{xx} (GPa) | σ_{yy} (GPa) | σ_{zz} (GPa) | $\mu_{\text{strained}}/\mu_{\text{unstrained}}$ |
|--------------------|--------------------|--------------------|---------------------|---------------------|---------------------|---|
| 1% | 0 | 0 | 1.66 | 0.641 | 0.641 | 1.37 |
| -1% | 0 | 0 | -1.66 | 0.641 | -0.641 | 0.32 |
| 1% | 1% | 0 | 2.30 | 2.30 | 1.28 | 1.40 |
| 1% | 0 | 1% | 2.30 | 1.28 | 2.30 | 1.37 |
| 0 | 1% | 1% | 1.28 | 2.30 | 2.30 | 0.36 |
| 0 | -1% | -1% | -1.28 | -2.30 | -2.30 | 1.31 |
| 1% | 1% | 1% | 2.94 | 2.94 | 2.94 | 1.05 |
| 1% | -1% | -1% | 0.377 | -1.66 | -1.66 | 1.36 |

Conclusion

We have spent considerable time in this class examining both the physics of semiconductors and the principles of operation of MOSFETs. Investigating the effects of

strain in theory and in simulation have helped me apply concepts which I learned in this course that were unfamiliar to me before, particularly concerning band structure and the effect strain has on it. I have also gained some practical knowledge of how device simulation can be performed. If time constraints were not an issue, I would have liked to have examined PMOS transistors in detail.

References

In addition to the references listed here, the lecture notes from this course were used.

1. Keyes, R. *Explaining Strain: The Positive and Negative Effects of Elastic Strain in n-Silicon*. IEEE Circuits and Devices Magazine (pp. 36-39.) (Sep. 2002)
2. Uchida, K., et al. *Physical Mechanisms of Electron Mobility Enhancement in Uniaxial Stressed MOSFETs and Impact of Uniaxial Stress Engineering in Ballistic Regime*. Electron Devices Meeting, 2005. IEDM Technical Digest, 5-7 Dec. 2005 (pp. 129-132.) (2005)
3. Everett, X.W., et al. *Physics of Hole Transport in Strained Silicon MOSFET Inversion Layers*. IEEE Transactions on Electron Devices, Vol. 53, No. 8. (2006)
4. *IBM's Strained Silicon Breakthrough Image Page*. Retrieved 16 Mar. 2007, from <http://www.research.ibm.com/resources/press/strainedsilicon/> (2001)
5. Wortman, J., et al. *Young's Modulus, Shear Modulus, and Poisson's Ratio in Silicon and Germanium*. Journal of Applied Physics, Vol. 36, No. 1. (1964)
6. Shah, N. *Stress Modeling of Nanoscale MOSFET*. MS Thesis, University of Florida. (2005)
7. *Sentaurus Device*. Version Y-2006.06. (2006)

Appendix A

All simulations were conducted using the “simple-Id-Vg” example as a starting point. The modified command file is included below for a particular simulation case.

```
File {
  * input files:
  Grid= "nmos_mdr.grd"
  Doping= "nmos_mdr.dat"
  * output files:
  Plot= "nl_des.dat"
  Current="nl_des.plt"
  Output= "nl_des.log"
}

Electrode {
  { Name="source" Voltage=0.0 }
  { Name="drain" Voltage=0.1 }
  { Name="gate" Voltage=0.0 Barrier=-0.55 }
  { Name="substrate" Voltage=0.0 }
}

Physics {
  Mobility( DopingDep HighFieldsat Enormal )
  EffectiveIntrinsicDensity( OldSlotboom )
}

Physics (Region = "Region 0") {
  Piezo(Stress = (-1.37e9, 0, -3.83e8, 0, 0, 0)
  OriKddX = (1,0,0)
  OriKddY = (0,1,0)
  Model(DeformationPotential Mobility(Subband)))
}

Plot {
  eDensity hDensity eCurrent hCurrent
  Potential SpaceCharge ElectricField
  eMobility hMobility eVelocity hVelocity
  Doping DonorConcentration AcceptorConcentration
  ElectrostaticPotential
}

Math {
  Extrapolate
  Derivatives
  NewDiscretization
}

Solve {
  Poisson
  #-initial solution:
  Coupled { Poisson Electron }
  #-ramp gate:
  Quasistationary ( MaxStep=0.05
    Goal { Name="gate" Voltage=2 } )
    { Coupled { Poisson Electron } }
  # ramp drain:
  Quasistationary ( MaxStep=0.05
    Goal { Name="drain" Voltage=5 } )
    { Coupled { Poisson Electron } }
}
```